

The Effect of Carbon Quantum Dots on *Candida* Species

Gamze Camlik^{1*}, Derya Doganay², Ibrahim Serkan Avsar³, Müzeyyen Aydın⁴, Ismail Tuncer Degim¹

¹Biruni University, Faculty of Pharmacy, Pharmaceutical Technology Department, Topkapi, 34015, Istanbul, Türkiye

²Saglik Bilimleri University, Faculty of Hamidiye Pharmacy, Pharmaceutical Microbiology, Uskudar, 34668, Istanbul, Türkiye

³Tokat Gaziosmanpasa University, Faculty of Pharmacy, Department of Pharmacology, Tokat, Türkiye

⁴Istanbul University, Faculty of Pharmacy, Department of Pharmaceutical Microbiology, 34126, Istanbul, Türkiye.

Corresponding Author: Gamze Camlik

Address: Department of Pharmaceutical Technology, Faculty of Pharmacy, Biruni University, Istanbul 34015, Türkiye.

Tel: 0 5469285606

E-mail: gcamlik@biruni.edu.tr

Key Words: *Candida*, carbon quantum dots, antifungal, fungal infection, antimicrobial resistance.

Application Date: 2025-06-05

Acceptance Date: 2025-07-03

ORCID IDs of the authors:

Gamze Camlik: 0000-0003-3282-8307

Derya Doğanay: 0000-0001-9147-4110

Ibrahim Serkan Avşar: 0000-0002-0343-8994

Müzeyyen Aydın: 0000-0002-8082-9470

Ismail Tuncer Degim: 0000-0002-9329-4698

Aim: Fungal resistance among *Candida* species limits antifungal efficacy, posing a global health threat. Due to increasing resistance and infection rates, this study explores carbon quantum dots (CQDs), synthesized with different heteroatom sources, as alternative antifungal agents against various *Candida* strains.

Materials and Methods: CQDs NaOH and CQDs EDA were synthesized and tested against six *Candida* strains using disk diffusion and Minimum Inhibitory Concentration (MIC) methods.

Results: Both CQDs formulations exhibited measurable antifungal activity against the tested *Candida* strains. Notably, CQDs EDA demonstrated superior antifungal efficacy compared to CQDs NaOH. Furthermore, the antifungal effect of CQDs EDA was more pronounced against clinical isolates relative to standard reference strains.

Conclusion: Incorporating various heteroatoms during CQDs synthesis alters key physicochemical properties such as surface chemistry, optical behavior and cellular interactions. These changes significantly impact antifungal activity against *Candida* spp. Thus, selecting suitable carbon sources and dopants is crucial for optimizing CQDs antifungal therapeutic potential.

Keywords: *Candida*, carbon quantum dots, antifungal, fungal infection, antimicrobial resistance

Introduction

Each year, more than 150 million cases of serious fungal infections (FIs) are reported globally, resulting in approximately 1.7 million deaths. Alarming, the number of cases continues to rise steadily. These infections represent a major global health burden, associated not only with high morbidity and mortality rates but also with severe socioeconomic consequences^{1–3}. Among fungal infections affecting large populations, candidiasis caused by species of the *Candida* genus is the most common. Although more frequently observed in immunocompromised individuals, candidiasis can also affect immunocompetent hosts. Candidemia (invasive candidiasis), an infection caused by *Candida* spp., is characterized as the most prevalent nosocomial fungal infection, exhibiting high mortality rates in immunocompromised patients.

Candida albicans remains the predominant clinical isolate and is considered the most frequently encountered and highly virulent fungal pathogen according to epidemiological surveillance data. However, the incidence of non-*albicans* *Candida* species such as *Candida parapsilosis*, *Candida tropicalis*, *Candida krusei*, *Candida glabrata*, *Candida guilliermondii*, *Candida orthopsilosis*, *Candida metapsilosis*, *Candida famata*, and *Candida lusitanae* has significantly increased, particularly among individuals infected with the human immunodeficiency virus (HIV)^{4–6}.

Azoles represent the most commonly prescribed class of antifungal medications currently available for managing *Candida* infections. Fluconazole is widely preferred among them due to its affordability and low toxicity profile. Nevertheless, the selection of antifungal therapy can vary depending on factors such as the infection site, type of *Candida* species involved, and their resistance patterns. Alternative classes like polyenes, echinocandins, nucleoside analogs, and allylamines may be considered in such cases⁷. A 2019 report from the Centers for Disease Control and Prevention (CDC) on antibiotic resistance highlighted that drug-resistant *Candida* species are linked to over 34,000 infections and around 1,700 deaths per year in the U.S. The report also categorized these resistant *Candida* strains as a “serious threat,” on par with the danger posed by methicillin-resistant *Staphylococcus aureus* (MRSA)⁸.

Traditional quantum dots (QDs), first described by L. Brus, are semiconductor nanocrystals composed of metals such as cadmium, selenium, and gold. These nanoparticles, typically 1–10 nm in size, exhibit unique fluorescence and size-dependent properties⁹. However, the metal-based nature of QDs raises significant toxicity concerns. In response, carbon quantum dots (CQDs) were developed in 2004, offering several advantages, including low toxicity, facile and cost-effective synthesis, high aqueous solubility, excellent biocompatibility, strong fluorescence quantum yield, and both excitation-dependent and independent emission properties. These features make CQDs highly attractive for applications in bioimaging, biosensing, drug delivery, and antimicrobial therapy. Additionally, understanding the quantum confinement effect and structural diversity of CQDs remains a key consideration in optimizing their performance¹⁰.

One of the most prominent features of CQDs is their antimicrobial activity, which is reported to be more structurally stable than that of conventional antibiotics¹¹. The primary antimicrobial mechanisms of CQDs involve the generation of reactive oxygen species (ROS), disruption of cell walls and membranes, and inhibition of gene expression¹². Due to their distinct mechanisms of action, CQDs show promise as antimicrobial agents, particularly against multidrug-resistant bacteria and fungi¹³. Moreover, their relatively low toxicity toward mammalian cells makes

them a compelling alternative to traditional antibiotics, with broad applications in antimicrobial research¹⁴.

In the present study, CQDs were synthesized via a microwave-assisted method using different heteroatom sources. Two formulations CQDs NaOH and CQDs ethylenediamine (EDA) were prepared, and their physicochemical properties (particle size, polydispersity index [PDI], and zeta potential) were characterized. Quantum yield (QY%) was also calculated. The antifungal activities of the CQDs were evaluated using disk diffusion and minimum inhibitory concentration (MIC) assays against *Candida* species, which are among the leading causes of fungal infections with increasing incidence and clinical significance.

Materials And Methods

Materials

Citric acid monohydrate (CAMH), sodium hydroxide (NaOH), and ethylene diamine (EDA) were obtained from Sigma Aldrich (Sigma Aldrich Chemie GmbH, Eschenstr. 5, 82024 Taufkirchen, Germany). L-cysteine was purchased from Biobasic (20 Konrad Crescent, Markham ON, L3R 8T4, Canada). All solutions were prepared using analytical-grade distilled water. Carbon quantum dots (CQDs) were synthesized using a microwave reactor (Microwave 300, Anton Paar, St. Albans, Hertfordshire, AL4 0LA, UK). Particle size, polydispersity index (PDI), and zeta potential were measured using an Anton Paar LiteSizer 500 instrument.

Test Microorganisms

The antifungal activity of the CQDs was evaluated against six *Candida* strains: four reference strains (*Candida albicans* ATCC (American Type Culture Collection) 10231, *Candida albicans* ATCC 1323, *Candida tropicalis* ATCC 750, and *Candida parapsilosis* ATCC 22019) and two clinical isolates (*C. albicans* and *C. parapsilosis*).

Synthesis of Carbon Quantum Dots (CQDs)

Two types of CQDs, designated as CQDs NaOH and CQDs EDA, were synthesized via microwave-assisted methods¹⁵. In both formulations, citric acid monohydrate served as the carbon source, while L-cysteine and ethylenediamine were used for surface passivation. The reactants were dissolved in 1 mL of distilled water and subjected to microwave irradiation at 140°C for 20 minutes.

The resulting CQDs exhibited characteristic blue fluorescence emission under 365 nm UV light, indicating successful formation. The pH of the L-cysteine containing CQDs was initially measured at 2–3; these were subsequently neutralized and purified with NaOH to yield physiologically compatible CQDs NaOH (pH 7–8). The CQDs synthesized with EDA (CQDs EDA) exhibited a pH within the physiological range (7–8) immediately after synthesis.

Characterization of CQDs NaOH and CQDs EDA

Particle Size (PS), Polydispersity Index (PDI), and Zeta Potential (ZP)

The particle size, PDI, and zeta potential of CQDs NaOH and CQDs EDA were measured using the Anton Paar LiteSizer 500. Each measurement was repeated ten times to ensure reproducibility.

Fluorescence and Quantum Yield (%)

Fluorescence properties of both CQDs NaOH and CQDs EDA were assessed under 365 nm UV light. QY% was calculated based on the following formula:

$$QY_c = QY_s \times (I_c / I_s) \times (A_s / A_c) \times (\eta_c / \eta_s)^2$$

QY%; represents the yield of carbon-based quantum dots, QY_s; represents the quantum yield of the reference quinine sulfate (0.54), I represents the fluorescence area, A; absorbance intensity at 360 nm excitation wavelength, η ; represents the refractive index, c; represents carbon-based quantum dots, and s; represents quinine sulfate¹⁶.

Antifungal Activity Assessment

Disk Diffusion Assay

Antifungal activity of CQDs was evaluated using the disk diffusion method on Mueller-Hinton Agar (MHA). A fungal suspension adjusted to 0.5 McFarland standard (10⁸ CFU/mL) was prepared using Mueller-Hinton Broth (MHB) after reviving the stored strains on Sabouraud Dextrose Agar (SDA). Disks impregnated with 20 μ L of each CQD formulation were placed on inoculated agar plates and incubated at 27°C for 18–24 hours. The diameter of the inhibition zones was measured in millimeters using a digital caliper. Voriconazole was used as the positive control. All experiments were conducted in triplicate¹⁷.

Minimum Inhibitory Concentration (MIC) Assay

The MIC values of CQDs were determined using the broth microdilution method in sterile, flat-bottomed 96-well microtiter plates (Brand). Fifty microliters of RPMI medium were added to all wells except the first column. In wells 1 and 2, 50 μ L of CQDs solution was added, and serial two-fold dilutions were made from well 2 to well 11 to achieve concentrations ranging from 50 μ L/mL to 0.097 μ L/mL (v/v). Fifty microliters of fungal suspension (10⁸ CFU/mL) were then added to all wells. The final well was left without CQDs as the growth control. A parallel setup using voriconazole (1000–0.5 μ g/mL) served as the control. All plates were incubated at 37°C for 24 hours.

Following incubation, 50 μ L of a 2 mg/mL solution of 2,3,5-triphenyl tetrazolium chloride (TTC, Merck) was added to each well and incubated for an additional 30 minutes. Color changes were assessed, and the lowest concentration that showed no visible growth was recorded as the MIC. All experiments were performed in triplicate¹⁷.

Ethical Considerations

This study does not involve human or animal subjects and therefore does not require ethical committee approval.

Statistical Analysis

Data were expressed as mean \pm standard deviation. The number of replicates (n) was indicated. Two-way ANOVA was used for statistical analysis.

Results

Synthesis of CQDs

CQDs NaOH and CQDs EDA synthesized via the microwave-assisted method exhibited characteristic blue fluorescence under 365 nm UV illumination. The final pH of the CQDs purified with NaOH was adjusted to a physiological range (pH 7–8). Similarly, the pH of CQDs EDA was found to be inherently within the physiological range (pH 7–8) without requiring additional adjustment.

Characterization of CQDs NaOH and CQDs EDA

Particle size (PS), polydispersity index% (PDI%), and zeta potential (ZP)

An Anton Paar LiteSizer 500 was used to measure the PS, PDI% and ZP values of the produced CQDs NaOH and CQDs EDA. The obtained measurement results are included in [Table 1](#).

Table 1. Particle size, polydispersity index (PDI%), and zeta potential (ZP) values of CQDs NaOH and CQDs EDA.

Fluorescence and QY%

CQDs NaOH and CQDs EDA showed blue fluorescence under 365 nm ultraviolet (UV) light ([Figure 1](#)). The QY% of CQDs NaOH and CQDs EDA were calculated to be 90.25% and 89.75%, respectively.

Figure 1. Fluorescence properties of CQDs NaOH (A) and CQDs EDA (B) under 365 nm UV light.

Antibacterial Activity

In this study, the antifungal activity findings of two different carbon quantum dots (CQDs NaOH and CQDs EDA), obtained from the Department of Pharmaceutical Technology, Faculty of Pharmacy, Biruni University, were evaluated against six *Candida** strains and are presented below ([Figure 2](#), [Table 2](#)).

Disk Diffusion Assay Results of the CQDs

Figure 2: Inhibition zone diameters of CQDs and voriconazole against yeasts.

Based on the findings of the study, both types of CQDs demonstrated inhibitory zone formation against the yeast strains, with varying diameters depending on the strain. CQDs EDA exhibited the most pronounced antifungal effect against *Candida parapsilosis* (clinical isolate), producing a 20 mm inhibition zone, while CQDs NaOH showed its highest activity against *Candida albicans* ATCC 10231, with a 10 mm zone.

Furthermore, analysis of the disk diffusion results for *C. albicans* ATCC 10231 and *C. albicans* ATCC 13231 revealed that CQDs EDA demonstrated the highest inhibitory activity (12 mm and 10 mm, respectively), with effects comparable to the positive control, voriconazole (15 mm and 12 mm, respectively).

In the case of *Candida tropicalis* ATCC 750, CQDs EDA produced a 15 mm inhibition zone, although this was considerably lower than that of the positive control (33 mm), indicating a relatively weaker antifungal effect for this strain.

Microdilution Assay Results of the CQDs

Table 2. Minimum Inhibitory Concentrations (MICs) of Carbon Quantum Dots (CQDs) and Voriconazole Against Yeast Strains

The MIC values of CQDs NaOH against the tested *Candida* strains ranged from ≥ 1 $\mu\text{L/mL}$ to 1 $\mu\text{L/mL}$, whereas those of CQDs EDA varied between 0.13 $\mu\text{L/mL}$ and 0.5 $\mu\text{L/mL}$. When the antifungal activity was evaluated based on MIC values, the lowest MIC for CQDs NaOH was found to be 0.5 $\mu\text{L/mL}$ (25% v/v) against *Candida tropicalis* ATCC 750. In contrast, the lowest MIC value for CQDs EDA was 0.13 $\mu\text{L/mL}$ (6.25% v/v), observed against *Candida tropicalis* ATCC 750, *Candida albicans* (clinical), and *Candida parapsilosis* (clinical).

Overall, the MIC results indicate that CQDs EDA exhibited greater antifungal activity than CQDs NaOH. In agreement with the disk diffusion findings, CQDs EDA consistently showed superior inhibitory effects. Additionally, CQDs EDA demonstrated stronger activity against the clinical isolates than against the reference strains.

Discussion

In this study, CQDs were successfully synthesized using a microwave-assisted bottom-up approach. The microwave synthesis method was chosen due to its advantages, including short reaction time, reproducibility, cost-effectiveness, environmental friendliness, and high efficiency^{18,19}. Initial assessment under 365 nm UV light revealed that both formulations exhibited characteristic blue fluorescence, which serves as a primary and rapid indicator of successful CQD formation²⁰.

CQDs are semiconductor nanocrystals with particle sizes below 10 nm that exhibit fluorescent properties²¹. In this study, the prepared CQDs had particle sizes below 2 nm, confirming their quantum behavior and successful synthesis (Table 1). The fluorescence color and intensity of CQDs may vary depending on surface defects, particle size, and structural damage. Unlike conventional QDs, where emission is strictly size-dependent, CQDs also exhibit fluorescence variations due to surface roughness. Particle size and surface functional groups play key roles in determining emission wavelength and intensity. Although larger particles tend to emit red light, this is not always the case in CQDs. Emission characteristics are also influenced by functional groups and heteroatoms incorporated during synthesis^{21,22}.

CQDs synthesized using nitrogen-containing molecules like L-cysteine and EDA emit blue fluorescence under UV light; however, when synthesized in neutral to slightly basic conditions, green emission can occur. This is due to the activation of nitrogen atoms under acidic conditions, which are incorporated into the CQD core, whereas in basic environments, sulfur atoms become active and serve as co-dopants altering surface properties and emission behavior.

Citric acid monohydrate (CAMH) was used as the carbon source in both formulations, while L-cysteine and EDA were selected as heteroatom dopants. Although the quantity of reactants used was found to be influential, it was not critical; variations led to reduced quantum yields, confirming the chosen concentrations as optimal. Other combinations tested did not yield superior results.

The CQDs prepared with CAMH and L-cysteine initially exhibited low pH values and were purified with NaOH to adjust their pH to a physiologically acceptable range (pH 7–8), resulting in CQDs NaOH. In alkaline conditions, citric acid converts to sodium citrate, which precipitates easily due to reduced solubility and larger crystal size, facilitating its removal¹⁵. CQDs synthesized using CAMH and EDA (CQDs EDA) naturally exhibited pH values within the physiological range.

In addition to particle size, PDI and zeta potential (ZP) values are critical characterization parameters. The PDI and ZP values for CQDs NaOH and CQDs EDA were determined as $15.24 \pm 0.18\%$ and $18.62 \pm 0.27\%$, and 12.43 ± 0.31 mV and 14.81 ± 0.21 mV, respectively. A low PDI% indicates a narrow and uniform particle size distribution^{22,23}. Zeta potential reflects surface charge and directly influences colloidal stability and interaction with biological systems²⁴. High absolute ZP values are associated with reduced aggregation and enhanced long-term colloidal stability, which are desirable for biomedical applications²⁰.

QY% is a key parameter in characterizing CQDs. Calculated using quinine sulfate as a standard fluorophore, both CQDs NaOH and CQDs EDA demonstrated high QY values of 90.25% and 89.75%, respectively, emitting bright blue fluorescence ([Figure 1](#)), further confirming the effectiveness of the synthesis protocol¹⁶.

Surface passivation with nitrogen groups can alter CQD surface charge, enhancing electrostatic interactions with negatively charged fungal cell walls. This improves CQD–cell interactions, possibly enhancing antifungal activity²⁵. Moreover, nitrogen dopants may increase the production of reactive oxygen species (ROS), which contribute to membrane damage and cell death^{26,27}. These dopants can also inhibit fungal biofilm formation complex, resistant structures that limit antifungal treatment efficacy^{28–30}.

CQDs have become promising nanomaterials in biomedical research, particularly for imaging and tracking cellular interactions. Their low cytotoxicity and high biocompatibility make them suitable for use in microbial models, including *Candida albicans*^{30,31}. Importantly, CQDs have been employed in visualizing drug–pathogen interactions, hyphal development, and distinguishing between drug-resistant and sensitive strains using confocal and atomic force microscopy^{32,33}.

In this study, the results obtained from both disk diffusion and microdilution methods were largely consistent. However, some discrepancies were observed. For instance, certain strains that showed no inhibition zones in the disk diffusion test yielded MIC values in the microdilution assay. This could be attributed to factors such as direct microorganism–CQD contact in the broth, agar composition, inoculum density, and diffusion characteristics of the material in solid media. Cadirci *et al.* (2005) reported that the microdilution method offers more precise and reliable results than the disk diffusion method for antimicrobial activity testing.³⁴ As such, some guidelines (e.g., Clinical & Laboratory Standards Institute (CLSI) M07-A8, 2009; CLSI M100, 2021) recommend broth microdilution as the standard method for clinical susceptibility testing.

When comparing the antifungal efficacy of CQDs NaOH (prepared using L-cysteine) and CQDs EDA (prepared using ethylenediamine), both demonstrated antifungal activity against the yeast strains; however, CQDs EDA was consistently more effective in terms of inhibition zone size and MIC values.

Various studies have explored the use of different carbon sources such as glucose, fructose, and polyethylene glycol (PEG) for CQD synthesis. CQDs offer versatility in synthesis routes

and materials, attracting increasing interest due to their biocompatibility, low toxicity, and antimicrobial potential³⁵. The antimicrobial activity of CQDs is believed to occur through three primary mechanisms: disruption of the cell membrane/wall, ROS generation, and binding to nucleic acids, thereby inhibiting cell replication.

Although the exact mechanisms remain to be fully elucidated, experimental findings strongly support the potential of CQDs as a novel class of antimicrobial agents.³⁶ Tirado-Guizar *et al.* (2023) investigated CdTe QDs and their Cu- and Ag-doped derivatives, reporting MIC values of 10–20 mg/L for *C. albicans* ATCC 10231 and 10–50 mg/L for *C. tropicalis* ATCC 750³⁷. Ezati *et al.* (2022) examined glucose-derived CQDs and their B-, S-, and N-doped variants, finding MIC values of 0.019–0.156 mg/mL for *Aspergillus fumigatus* and 0.027–0.312 mg/mL for *C. albicans*³⁸. Chand *et al.* (2021) evaluated ZnO QDs against *C. albicans* isolates, reporting MICs ranging from 0 to 0.2 mg/mL³⁹. These findings further highlight the growing interest in QDs for antifungal applications.

Recent studies also emphasize the potential of CQDs to prevent *Candida* biofilm formation and adhesion key processes contributing to antifungal resistance thus offering promising alternatives for treatment^{38–40}.

The results of the current study are consistent with the literature. One of the distinctive features of this study is the use of CAMH as a carbon source. CAMH's acidic nature may confound antimicrobial efficacy by altering the final pH of the solution. Thus, we purified and neutralized the CQDs NaOH to isolate the true activity of the CQDs from any pH-related effects¹⁵. Furthermore, the use of different heteroatom sources significantly influenced the physicochemical properties of the CQDs including surface chemistry, optical behavior, and stability affecting their biological performance⁴². Heteroatoms can alter band gaps and emission wavelengths; for instance, nitrogen-doped CQDs typically emit blue light, while sulfur-doped ones emit at longer wavelengths^{42,43}. They also contribute to the formation of functional groups that improve solubility, biocompatibility, and molecular interactions⁴⁴.

Conclusion

In conclusion, CQDs NaOH and CQDs EDA were successfully synthesized using different heteroatom sources. Both formulations were fully characterized and exhibited high quantum yields. Their antifungal activity against six *Candida* strains demonstrated that heteroatom composition significantly influenced biological efficacy. This study confirms the potential of CQDs as promising antifungal agents and highlights the critical role of heteroatom selection in tailoring CQD functionality for specific applications.

Moreover, this work provides a foundational basis for future studies exploring the synergistic effects of CQDs in combination with conventional antifungal agents.

Ethics Committee Approval: This article does not contain any studies with human or animal subjects.

Author Contributions: G.C., I.T.D., and D.D. conceived and designed the study. G.C. and M.A. performed the experiments and collected the data. I.T.D., I.S.A., G.C., and D.D analyzed and interpreted the data. I.S.A. and G.C. wrote the initial draft of the manuscript. All authors reviewed and revised the manuscript critically.

Acknowledgments: There are no acknowledgements to declare.

Conflict of Interest: The authors declare that there is no conflict of interest.

References

1. Kainz K, Bauer MA, Madeo F, Carmona-Gutierrez D. Fungal infections in humans: the silent crisis. *Microb Cell*. 2020;7(6):143–5.
2. World Health Organization. Global Tuberculosis Report. https://www.who.int/tb/publications/global_report/en/, Accessed 15..
3. World Health Organization. World Malaria Report. <https://www.who.int/publications-detail/world-malaria-report-2019>, Accessed 15.05.2020.
4. Barchiesi F, Orsetti E, Osimani P, Catassi C, Santelli F, Manso E. Factors related to outcome of bloodstream infections due to *Candida parapsilosis* complex. *BMC Infect Dis*. 2016;16(1):387.
5. Lewis LE, Bain JM, Lowes C, Gow NAR, Erwig LP. *Candida albicans* infection inhibits macrophage cell division and proliferation. *Fungal Genet Biol*. 2012;49(9):679–80.
6. Ferreira AV, Prado CG, Carvalho RR, Dias KST, Dias ALT. *Candida albicans* and Non-*C. albicans* *Candida* Species: Comparison of Biofilm Production and Metabolic Activity in Biofilms, and Putative Virulence Properties of Isolates from Hospital Environments and Infections. *Mycopathologia*. 2013;175(3–4):265–72.
7. Pfaller MA, Castanheira M, Messer SA, Moet GJ, Jones RN. Variation in *Candida* spp. distribution and antifungal resistance rates among bloodstream infection isolates by patient age: report from the SENTRY Antimicrobial Surveillance Program (2008–2009). *Diagn Microbiol Infect Dis*. 2010;68(3):278–83.
8. Fang Y, Guo S, Li D, et al. Easy Synthesis and Imaging Applications of Cross-Linked Green Fluorescent Hollow Carbon Nanoparticles. *ACS Nano*. 2012;6(1):400–9.
9. Camlik G, Bilakaya B, Uyar P, Degim Z, Degim IT. New generation of composite carbon quantum dots for imaging, diagnosing, and treatment of cancer. In: *Functionalized Nanomaterials for Cancer Research*. Elsevier; 2024:543–57.
10. Lim SY, Shen W, Gao Z. Carbon quantum dots and their applications. *Chem Soc Rev*. 2015;44(1):362–81.
11. Najmaldin Ghaibullah Ghaibullah Y, Foto E, Ozdemir N, Zilifdar Foto F, Arslan G, Sargin I. Antibacterial potentials of carbon dots immobilized on chitosan and glass surfaces. *Int J Biol Macromol*. 2024;257:128586.
12. Wu Y, Li C, van der Mei HC, Busscher HJ, Ren Y. Carbon Quantum Dots Derived from Different Carbon Sources for Antibacterial Applications. *Antibiotics*. 2021;10(6):623.
13. Guo B, Liu G, Hu C, Lei B, Liu Y. The structural characteristics and mechanisms of antimicrobial carbon dots: a mini review. *Mater Adv*. 2022;3(21):7726–41.
14. Abbas K, Zhu H, Qin W, Wang M, Li Z, Bi H. Enhanced Antibacterial Activity of Carbon Dots: A Hybrid Approach with Levofloxacin, Curcumin, and Tea Polyphenols. *C (Basel)*. 2024;10(3):84.
15. Camlik G, Bilakaya B, Ozsoy Y, Degim IT. A new approach for the treatment of Alzheimer’s disease: insulin-quantum dots. *J Microencapsul*. 2024;41(1):18–26.
16. Xue H, Yan Y, Hou Y, Li G, Hao C. Novel carbon quantum dots for fluorescent detection of phenol and insights into the mechanism. *New J Chem*. 2018;42(14):11485–92.
17. Clinical and Laboratory Standards Institute. M100 Performance Standards for Antimicrobial Susceptibility Testing. 32nd Edition. Vol. 42.
18. Camlik G, Ozakca I, Bilakaya B, et al. Development of composite carbon quantum dots-insulin formulation for oral administration. *J Drug Deliv Sci Technol*. 2022;76:103833.
19. Jamkhane PG, Ghule NW, Bamer AH, Kalaskar MG. Metal nanoparticles synthesis: An overview on methods of preparation, advantages and disadvantages, and applications. *J Drug Deliv Sci Technol*. 2019;53:101174.
20. Zaini MS, Jian LY, Liew JYC, Kamarudin MA. Impact of carbon concentration on optical and zeta potential properties of carbon quantum dots. *Fullerenes Nanotubes Carbon Nanostruct*. 2024;32(11):1039–49.
21. Camlik, G., Bilakaya, B., Güven, G. K., Akkol, E. K., Degim, Z., Sobarzo-Sánchez, E., & Degim, I. T. Quantum Drugs (Q-Drugs): A New Discovery and Taboo Breaking Approach; Producing Carbon Quantum Dots from Drug Molecules. *Pharmaceutics* 2025;18(6):767.
22. Hoseini B, Jaafari MR, Golabpour A, Momtazi-Borojeni AA, Karimi M, Eslami S. Application of ensemble machine learning approach to assess the factors affecting size and polydispersity index of liposomal nanoparticles. *Sci Rep*. 2023;13(1):18012.
23. Danaei M, Dehghankhold M, Ataei S, et al. Impact of Particle Size and Polydispersity Index on the Clinical Applications of Lipidic Nanocarrier Systems. *Pharmaceutics*. 2018;10(2):57.



24. Moore TL, Rodriguez-Lorenzo L, Hirsch V, et al. Nanoparticle colloidal stability in cell culture media and impact on cellular interactions. *Chem Soc Rev*. 2015;44(17):6287–305.
25. Sheikh MA, Chandok RS, Abida K. High energy density storage, antifungal activity and enhanced bioimaging by green self-doped heteroatom carbon dots. *Discover Nano*. 2023;18(1):132.
26. Li Q, Shen X, Xing D. Carbon quantum dots as ROS-generator and -scavenger: A comprehensive review. *Dyes Pigments*. 2023;208:110784.
27. Wang L, Wang T, Hao R, Wang Y. Construction Strategy and Mechanism of a Novel Wood Preservative with Excellent Antifungal Effects. *Molecules*. 2024;29(5):1013.
28. Sturabotti E, Camilli A, Moldoveanu VG, et al. Targeting the Antifungal Activity of Carbon Dots against *Candida albicans* Biofilm Formation by Tailoring Their Surface Functional Groups. *Chem Eur J*. 2024;30(18).
29. Pereira R, Santos Fontenelle RO, Brito EHS, Morais SM. Biofilm of *Candida albicans*: formation, regulation and resistance. *J Appl Microbiol*. 2021;131(1):11–22.
30. Cui F, Ning Y, Wang D, Li J, Li X, Li T. Carbon dot-based therapeutics for combating drug-resistant bacteria and biofilm infections in food preservation. *Crit Rev Food Sci Nutr*. 2024;64(2):203–19.
31. Rajendiran K, Zhao Z, Pei DS, Fu A. Antimicrobial Activity and Mechanism of Functionalized Quantum Dots. *Polymers (Basel)*. 2019;11(10):1670.
32. Rais A, Sharma S, Mishra P, Khan LA, Prasad T. Biocompatible Carbon Quantum Dots as Versatile Imaging Nanotrackers of Fungal Pathogen – *Candida Albicans*. *Nanomedicine*. 2024;19(8):671–88.
33. Jiang Y, Yin C, Mo J, et al. Recent progress in carbon dots for anti-pathogen applications in oral cavity. *Front Cell Infect Microbiol*. 2023;13.
34. Hilal Cadi B, Citak S. A Comparison of Two Methods Used for Measuring Antagonistic Activity of Lactic Acid Bacteria. *Pakistan J Nutr*. 2005;4(4):237–41.
35. Pourmadadi M, Rahmani E, Rajabzadeh-Khosroshahi M, et al. Properties and application of carbon quantum dots (CQDs) in biosensors for disease detection: A comprehensive review. *J Drug Deliv Sci Technol*. 2023;80:104156.
36. Hussen NH, Hasan AH, FaqiKhedr YM, Bogoyavlenskiy A, Bhat AR, Jamalis J. Carbon Dot Based Carbon Nanoparticles as Potent Antimicrobial, Antiviral, and Anticancer Agents. *ACS Omega*. 2024;9(9):9849–64.
37. Tirado-Guizar A, Pina-Luis GE, Trujillo-Navarrete B, Paraguay-Delgado F. Copper and silver doped in CdTe quantum dots: *C. albicans* and *C. tropicalis* antifungal nanomaterials. *Mater Res Express*. 2023;10(4):045003.
38. Ezati P, Rhim JW, Molaei R, et al. Preparation and characterization of B, S, and N-doped glucose carbon dots: Antibacterial, antifungal, and antioxidant activity. *Sustain Mater Technol*. 2022;32:e00397.
39. Chand P, Kumari S, Mondal N, Singh SP, Prasad T. Synergism of Zinc Oxide Quantum Dots with Antifungal Drugs: Potential Approach for Combination Therapy against Drug Resistant *Candida albicans*. *Front Nanotechnol*. 2021;3.
40. Priyadarshini E, Rawat K, Prasad T, Bohidar HB. Antifungal efficacy of Au@ carbon dots nanoconjugates against opportunistic fungal pathogen, *Candida albicans*. *Colloids Surf B Biointerfaces*. 2018;163:355–61.
41. Kostov K, Andonova-Lilova B, Smagghe G. Inhibitory activity of carbon quantum dots against *Phytophthora infestans* and fungal plant pathogens and their effect on dsRNA-induced gene silencing. *Biotechnol Biotechnol Equip*. 2022;36(1):949–59.
42. Kong J, Wei Y, Zhou F, et al. Carbon Quantum Dots: Properties, Preparation, and Applications. *Molecules*. 2024;29(9):2002.
43. Tiras KS, Soheyli E, Sharifirad Z, Mutlugun E. Optimization of high efficiency blue emissive N-, S-doped graphene quantum dots. *Opt Mater*. 2025;159:116544.
44. Azami M, Wei J, Valizadehderakhshan M, Jayapalan A, Ayodele OO, Nowlin K. Effect of Doping Heteroatoms on the Optical Behaviors and Radical Scavenging Properties of Carbon Nanodots. *J Phys Chem C*. 2023;127(15):7360–70.

Table 1. Particle size, polydispersity index (PDI%), and zeta potential (ZP) values of CQDs NaOH and CQDs EDA.

	Particle Size (nm)	Polydispersity Index% (PDI%)	Zeta Potantial (mV)
CQDs NaOH	1.62 ± 0.23	15.24 ± 0.18	12.43 ± 0.31
CQDs EDA	1.78 ± 0.14	18.62 ± 0.27	14.81 ± 0.21

Table 2. Minimum Inhibitory Concentrations (MICs) of Carbon Quantum Dots (CQDs) and Voriconazole Against Yeast Strains

Microorganisms												
	<i>Candida albicans</i> ATCC 13231		<i>Candida albicans</i> ATCC 10231		<i>Candida albicans</i> (clinic)		<i>Candida tropicalis</i> ATCC 750		<i>Candida parapsilosis</i> ATCC 22019		<i>Candida parapsilosis</i> (klinik)	
Formulations	MIC (µl/mL)	MIC (%) v/v	MIC (µl/mL)	MIC (%) v/v	MIC (µl/mL)	MIC (%) v/v	MIC (µl/mL)	MIC (%) v/v	MIC (µl/mL)	MIC (%) v/v	MIC (µl/mL)	MIC (%) v/v
CQDs NaOH	1	50%	1	50%	≥1	≥50%	0,5	25%	≥1	≥50%	≥1	≥50%
CQDs EDA	0.5	25%	0.5	25%	0.13	6.25%	0.13	6.25%	0.5	25%	0.13	6.25%
Voriconazole	500 (µg/mL)		250 (µg/mL)		62.5 (µg/mL)		3.25 (µg/mL)		1000 (µg/mL)		62.5 (µg/mL)	

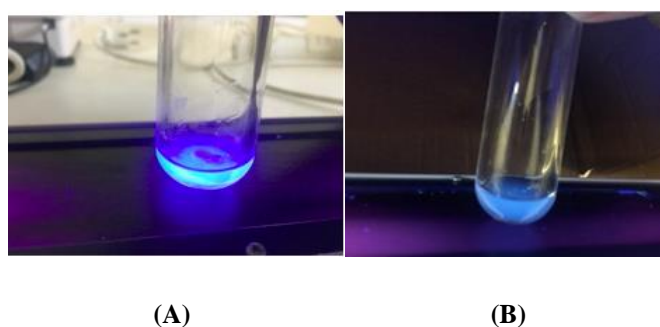


Figure 1. Fluorescence properties of CQDs NaOH (A) and CQDs EDA (B) under 365 nm UV light.

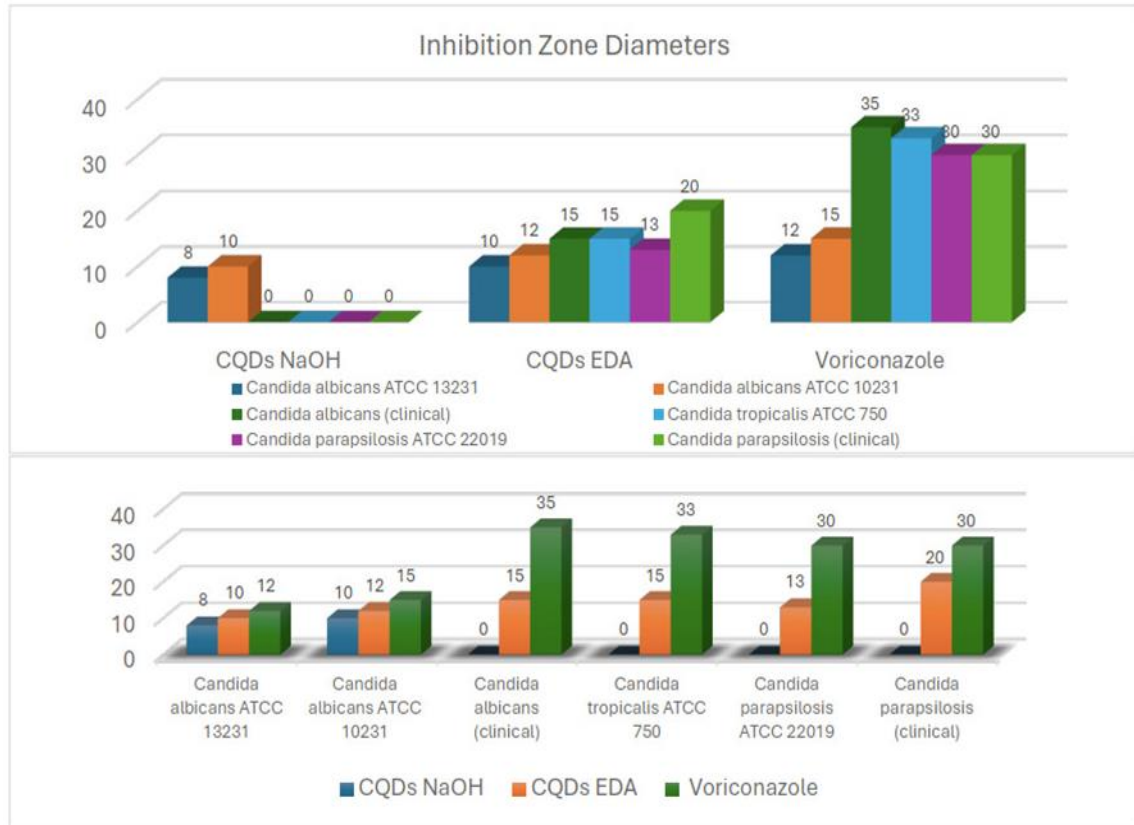


Figure 2. Inhibition zone diameters of CQDs and voriconazole against yeasts.